Reprint

An Instrument for Real-time Emulation of Multipath Fading in Indoor Power-Line Networks

D. Anastasiadou, P. Savvopoulos and T. Antonakopoulos

IEEE Instrumentation and Measurement Technology Conference, IMTC-2003

VAIL-COLORADO, USA, MAY 2003

An Instrument for Real-Time Emulation of Multipath Fading in Indoor Power-Line Networks

Despina Anastasiadou[1], Panayiotis Savvopoulos[2] and Theodore Antonakopoulos[2]

[1] Academic Research Computers Technology Institute
61 Riga Feraiou Str., 26100 Patras, Greece
Phone: +30-2610-996-489, Fax: +30-2610-997-342, Email: Despina.Anastasiadou@cti.gr
[2] Department of Electrical Engineering and Computers Technology
University of Patras, Rio, Patras, 26500, Greece
Phone: +30-2610-996-487, Fax: +30-2610-997-342, Email: antonako@ee.upatras.gr

Abstract – This paper presents an instrument for real-time emulation of any power-line network topology. The instrument is based on the analytical computation of transmission channel characteristics and the accurate description of its multipath behavior utilizing information, such as wiring cable dimensions, nodes' interconnectivity and termination load impedances. The presented instrument also supports real-time adaptation of its configuration parameters in order to emulate the time varying behavior of the power-line channel. As the comparative analysis demonstrates, there is satisfactory convergence between theoretical and experimental results.

I. INTRODUCTION

The idea of utilizing the indoor power distribution infrastructure in order to provide high speed networking services at every AC outlet inside common residential and commercial buildings has been investigated intensely during the last few years. Recent results agree that broadband communications on power-line channels are feasible with data rates in the Mbps range [1]. The design of reliable power-line communications (PLC) systems requires detailed knowledge of the channel characteristics, while performance testing and verification in various network topologies and loading[1] conditions requires the use of flexible and accurate channel emulation.

The power distribution network constitutes a rather hostile environment due to multipath fading caused by impedance mismatching, and also due to noise introduced by various sources. The channel also exhibits time-varying characteristics caused by loads either being connected and disconnected from the network or having time varying behavior, thus changing the channel response. Numerous efforts have been made to measure and statistically characterize the time and frequency varying behavior of the power grid [2], [3], although a widely accepted channel model has not yet been presented. A common modelling approach considers the channel as a 'black box' and extracts a number of system parameters from measurement results [4]. Using the same approach, the channel has been examined as a multipath environment, whose characteristics can be determined using experimental measurements [5].

---

[1] The impedances of the loads connected at every network termination point are also being referred to as network loading conditions.

Furthermore, the development of PLC systems requires the use of a reliable and flexible test-bench, before performance tests can be executed on actual indoor power-line networks. A number of non real-time simulators have been proposed in the literature [6], in addition to a hardware emulator, whose configuration parameters were derived from measurements on several reference channels [7].

Taking a different approach, this work presents an instrument for real-time emulation of power-line networks that can be used to evaluate the performance of power-line transmission techniques on any network topology. The main advantage of such an instrument is that its functionality is based on the analytical computation of the channel transmission characteristics and the accurate description of its multipath behavior. This instrument provides a very accurate approach for determining the transmission behavior of any network topology, thus it eliminates the need for setting up different experimental network configurations. Using information, such as wiring cable dimensions, node interconnectivity and termination load impedances, the transmission paths can be determined and the corresponding transmission parameters can be calculated, in order to configure the hardware emulation platform appropriately. The proposed instrument enables real-time adaptation of its configuration parameters in order to facilitate emulation of the time varying characteristics of the power-line channel.

The paper is organized in a manner that offers a comprehensive presentation of the emulator's design and implementation details. In Section II we give a concise description of the method that analytically computes the multipath characteristics of any power-line network. Section III describes the instrument's architecture and discusses the implementation details. Finally, a comprehensive example is analyzed in the Appendix to demonstrate the satisfactory convergence between theoretical and experimental results.

II. THE INDOOR POWERLINE MULTIPATH EFFECT

The indoor power-line grid can be considered as a multipath channel, since signal propagation between any transmitter-

receiver pair is performed through the shortest (direct) path and a large number of alternative paths. The transmitted signal suffers from amplitude and phase distortion due to line propagation and reflections at various channel discontinuities, such as cable junctions and termination impedances. As a result, replicas of the original signal reach the receiver with different amplitude and phase characteristics. However, unlike in the case of the open-air wireless environment, analytical calculation of the multipath effect in an indoor power-line network is feasible, due to its loop-free topology and its bounded complexity. Thus, multipath fading at the receiver can be traced back to the channel's physical characteristics and its termination impedances, by calculating cable loss, reflection and transmission coefficients.

Considering L different propagation paths between two communicating devices, the channel impulse response can be calculated as the sum of the received signal components, according to:

$$h(\tau, t) = \sum_{i=1}^{L} \{r_i e^{j\theta_i} . e^{-\alpha l_i} . \delta(t - \tau_i)\} \qquad (1)$$

where $r_i e^{j\theta_i}$ is the reflection factor of path i, $e^{-\alpha l_i}$ is the respective propagation factor, which depends on the path's length l_i and the line propagation constant $\gamma = \alpha + j\beta$, and $\tau_i = l_i/v$ is the path's delay, which additionally depends on the group velocity of propagation $v = \omega/\beta$.

In order to calculate the impulse response of every point-to-point connection on any power-line network, an efficient algorithm [8] has to be utilized, which analytically calculates the reflection factor, the propagation loss and the delay of every path in the frequency range of interest. The algorithm's input is a set of network description matrices that comprise information on the specific network structure, topology and loading. Thus, every indoor power-line network can be described by specifying its termination impedances, line section types and lengths and their connectivity. For each type of cable, the characteristic impedance Z_0 and the propagation constant γ can be measured or calculated through transmission line theory equations, using the cable primary parameters (R', L', C', G') [9], [10].

The reflection coefficients at every network point depend on the characteristic impedance Z_0 and the aggregate impedance Z_X seen by a signal reaching the corresponding point according to:

$$\rho = \frac{Z_0 + Z_X}{Z_0 - Z_X} \qquad (2)$$

Since Z_0 and γ are frequency dependent variables, the propagation loss factors and the reflection/transmission coefficients also vary with frequency. The reflection factor of a particular path is the product of all reflection/transmission coefficients that comprise the path and is thus frequency dependent, affecting both the signal's amplitude and phase. The following expression corresponds to the reflection factor of path i that

consists of M, not necessarily different, discontinuities:

$$r_i e^{j\theta_i} = \prod_{k=1}^{M} \{\rho_{ik}\} \qquad (3)$$

Considering the impulse response presented in (1), the channel's frequency response can be expressed as the sum of path-related and frequency dependent factors:

$$H(f) = \sum_{i=1}^{L} \{r_i e^{j\theta_i} . e^{-\gamma l_i}\} \qquad (4)$$

since $F\{\delta(t - \tau_i)\} = e^{-j\omega\tau_i} = e^{-j\omega l_i/v} = e^{-j\beta l_i}$, where F symbolizes the Fourier transform.

In order to offer a comprehensive description of the theoretical analysis we divide the frequency band of interest into a number of subchannels. The bandwidth of each subchannel is chosen so that the frequency response within the corresponding frequency range can be considered constant. Furthermore, we define the *path complex factor* that represents the amplitude and phase distortion of a signal frequency component on a particular path as:

$$pcf_{in} = r_{in} e^{j\theta_{in}} . e^{-\gamma_n l_i} = a_{in} e^{j\phi_{in}} \qquad (5)$$

where the i and n indices refer to the path and the frequency subchannel respectively. The term frequency component refers to a signal whose frequency content is limited to a single subchannel.

Therefore, every point-to-point connection on the power-line network can be characterized by a *path complex factor* matrix $\mathbf{PCF}[LxN]$:

$$\mathbf{PCF} = \begin{bmatrix} a_{11}e^{j\phi_{11}} & . & a_{1n}e^{j\phi_{1n}} & . & a_{1N}e^{j\phi_{1N}} \\ . & . & . & . & . \\ a_{i1}e^{j\phi_{i1}} & . & a_{in}e^{j\phi_{in}} & . & a_{iN}e^{j\phi_{iN}} \\ . & . & . & . & . \\ a_{L1}e^{j\phi_{L1}} & . & a_{Ln}e^{j\phi_{Ln}} & . & a_{LN}e^{j\phi_{LN}} \end{bmatrix}$$

where L is the number of significant paths between the transmitter and the receiver and N is the number of subchannels under consideration.

The sum of every column of the $\mathbf{PCF}$ matrix is the *total complex factor* that determines the amplitude and phase distortion of the respective signal frequency component, as defined in (6). This parameter is used to configure the emulator's hardware, described in the next section.

$$tcf_n = a_n e^{j\phi_n} = \sum_{i=1}^{L} \{a_{in} e^{j\phi_{in}}\} \qquad (6)$$

Before concluding the above theoretical analysis, the parameters' calculation process is demonstrated on the sample network presented in Fig. 1. The network is constructed using type H05VVF (3 x 1.5 mm^2) cables, with the characteristic impedance (Z_0) shown in Fig. 2. between 1 and 20 MHz.
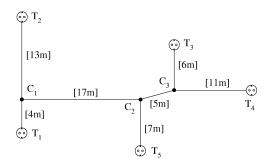
Fig. 1. An example for network analysis.

The network has $m = 5$ termination points (T_i) and $n = 3$ internal nodes (C_j) and it can be described using the following matrices:

$$\mathbf{TC} = \begin{bmatrix} 1 & 0 & 0 \\ 1 & 0 & 0 \\ 0 & 0 & 1 \\ 0 & 0 & 1 \\ 0 & 1 & 0 \end{bmatrix} \quad \mathbf{LT} = \begin{bmatrix} 4 & 0 & 0 \\ 13 & 0 & 0 \\ 0 & 0 & 6 \\ 0 & 0 & 11 \\ 0 & 7 & 0 \end{bmatrix}$$

$$\mathbf{CC} = \begin{bmatrix} 0 & 1 & 0 \\ 1 & 0 & 1 \\ 0 & 1 & 0 \end{bmatrix} \quad \mathbf{LC} = \begin{bmatrix} 0 & 17 & 0 \\ 17 & 0 & 5 \\ 0 & 5 & 0 \end{bmatrix}$$

The matrix $\mathbf{TC}$ describes the interconnections between termination points and nodes. Each line corresponds to a termination point T_i and each column to a node C_j. Element $TC(i, j)$ is equal to one when a connection between T_i and C_j exists, otherwise it is equal to zero. In the same manner, the $\mathbf{CC}$ matrix describes the interconnections between the internal network nodes. Since nodes cannot be connected to themselves and $C_i C_j = C_j C_i$, the $\mathbf{CC}$ matrix has zero diagonal and exhibits symmetry around it. The $\mathbf{LT}$ and $\mathbf{LC}$ matrices
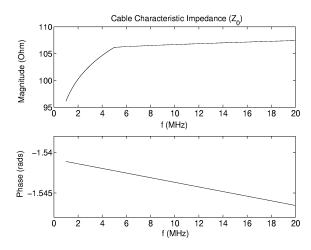

Fig. 2. H05VVF cable characteristic impedance in the frequency range of 1-20 MHz.

are generated by replacing the non-zero elements of $\mathbf{TC}$ and $\mathbf{CC}$ matrices with the respective lengths, $l_{T_i C_j}$ and $l_{C_i C_j}$.

Let us consider the channel transmission characteristics between termination points T_1 and T_4, when communication transceivers are connected at each termination point, with an impedance of 50 Ohms. The rows of the $\mathbf{PCF}$ matrix presented below, correspond to the first five significant paths, based on their propagation delay τ_i. The columns correspond to four consecutive subchannels of 50 KHz each, in the range of 8.0-8.2 MHz:

$$|\mathbf{PCF}| = \begin{bmatrix} 0.730 & 0.661 & 0.593 & 0.537 \\ 0.176 & 0.188 & 0.191 & 0.191 \\ 0.362 & 0.316 & 0.274 & 0.239 \\ 0.629 & 0.582 & 0.522 & 0.460 \\ 0.322 & 0.260 & 0.221 & 0.204 \end{bmatrix}$$

$$\angle\mathbf{PCF} = \begin{bmatrix} 131.9^o & 122.7^o & 115.8^o & 111.7^o \\ 8.5^o & -20.5^o & -44.0^o & -62.8^o \\ -47.9^o & -67.9^o & -86.1^o & -102.2^o \\ 88.9^o & 72.8^o & 58.7^o & 47.1^o \\ 19.9^o & 16.4^o & 17.5^o & 21.2^o \end{bmatrix}$$

Therefore, based on the $\mathbf{PCF}$ matrix the calculated *total complex factor* for the four subchannels is:

$$|tcf| = \begin{bmatrix} 1.068 & 0.901 & 0.744 & 0.611 \end{bmatrix}$$

$$\angle tcf = \begin{bmatrix} 176.8^o & 66.5^o & 59.3^o & 56.0^o \end{bmatrix}$$

If the impedance at the termination point T3 changes to 30 Ohms, then the PCF matrix changes and the corresponding *total complex factor* for the four subchannels becomes:

$$|tcf| = \begin{bmatrix} 1.166 & 1.038 & 0.904 & 0.773 \end{bmatrix}$$

$$\angle tcf = \begin{bmatrix} 91.6^o & 80.0^o & 69.8^o & 61.6^o \end{bmatrix}$$

III. THE EMULATOR'S ARCHITECTURE

The theoretical analysis indicates that the power-line channel exhibits frequency as well as time varying characteristics. Therefore, an efficient emulation instrument should satisfy the following requirements:

- Each signal frequency component must be affected by the corresponding amplitude and phase factors.
- The channel characteristics change as time progresses and therefore the emulator should be updated accordingly during real-time operation.

In order to comply with the first requirement, the emulator was designed to decompose the incoming signal into its frequency components and to filter each component using the appropriate bandpass FIR filter (BPF_i). The FIR coefficients of subchannel n can be derived from the $\mathbf{PCF}$ matrix using the elements of the respective column, after suitably transforming the inclusive delay factor $e^{-j\omega_n \tau_i}$ into the appropriate number
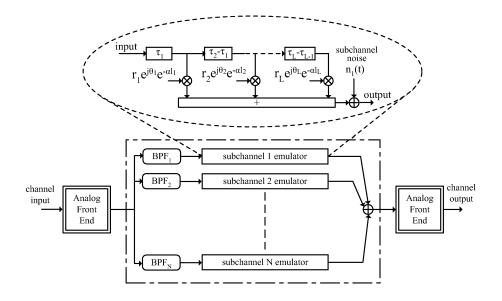
Fig. 3. The time domain architecture of the power-line emulation instrument.

of unit delay taps τ_s (sampling time). It is noted, that the two directions of transmission between any two communicating devices correspond to different **PCF** matrices and therefore the above implementation approach should be repeated to emulate both channel directions.

The emulator's architecture presented in Fig. 3. is the direct implementation of the above analysis. Unfortunately, it results to high order filters, since a large number of taps is required in order to emulate the propagation delays and to implement sharp bandpass filters for components' separation. Furthermore, this architecture limits the instrument's length discernibility, since the smallest emulated cable length has immediate bearing to the filters' order.

A more efficient design can be achieved by transforming the previous analysis in the frequency domain, as it is shown in Fig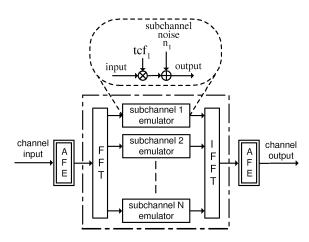. 4. The samples of the input signal are transformed into the frequency domain using FFT (Fast Fourier Transform) and each frequency component, that corresponds to a specific subchannel, is affected by the corresponding *total complex factor*. The order of the FFT has to be selected so that there is at least one frequency component per subchannel. At this stage the emulator can also insert noise into each subchannel, in order to emulate other sources of disturbance present in the power-line environment. At the end of this procedure, the frequency components are transformed back to the time domain using IFFT (Inverse Fast Fourier Transform). Thus, the subchannel filtering procedure is reduced to a complex multiplication. Moreover, this architecture has unlimited length discernibility, which was the main reason for selecting it for the emulator's implementation.

In order to satisfy the second requirement, the emulator uses a flexible interface for updating the operational *tcf* parameters during real-time operation. The emulator uses an internal table which contains all *tcf* parameters and is also accessible by an external host that can reconfigure its parameters according to the time varying loading conditions. Using multiple tables and the appropriate timing information, the emulator can be configured to emulate any time varying network behavior.

The power-line network emulator has been prototyped using two Virtex II FPGAs and a high performance DSP. A block diagram of the implemented emulator is shown in Fig. 5. The first FPGA is used in order to acquire the incoming data stream, to perform lowpass filtering (depending on the maximum frequency of interest) and to split the data into blocks of N-samples each, before they are processed by the FFT engine. The results of each FFT processing are stored in a dual-port RAM and the DSP is informed accordingly. The DSP multiplies the FFT components with the corresponding *tcf* parameters contained in its internal tables. At the last stage, the

Fig. 4. The frequency domain architecture of the power-line emulation instrument.
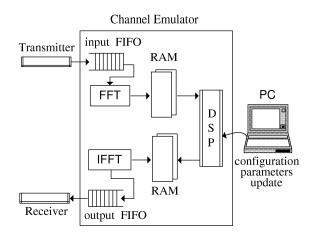
Fig. 5. Block diagram of the implemented real-time emulator.

DSP inserts noise into each subchannel and the results are stored at the output dual-port RAM. At this point, the IFFT engine, which is located at the second FPGA, is activated and the output data stream is generated. Additional functions, like decimation/interpolation at the emulator's input and the respective interpolation/decimation at its output, can also be performed for increasing the number of supported subchannels or for changing the subchannels' bandwidth.

In its current implementation, the emulator exchanges data at 20 MSamples/sec, on the level of its analog-front-end interfaces, while the transformation to and from the frequency domain is performed using 1024-points FFT and IFFT modules. As a result that the subchannel bandwidth is approximately 20 kHz. The DSP utilized operates at 150 MHz and the total time required for implementing the emulation of each subchannel is 840 nsec. Since the total acquisition time per FFT block is 51.2 usec, the emulator supports 50 subchannels simultaneously (taking into account some additional overhead), which equals to a total frequency range of 1 MHz.

IV. CONCLUSIONS

This paper presented an instrument for real-time emulation of power-line networks, which can be used to evaluate the performance of various transmission techniques on any network topology. This instrument is based on the analytical computation of transmission channel characteristics and the accurate description of the power-line network multipath behavior. The instrument can also support real-time adaptation of its configuration parameters in order to facilitate emulation of the time varying behavior of the power-line channel.

V. ACKNOWLEDGMENTS

VI. APPENDIX

In this Appendix we demonstrate the mechanism of signal propagation using a comprehensive example of a single line of length l and validate the theoretical analysis by comparing theoretical and measurement results. The measurement setup consists of the line segment, the signal generator and the termination loads (Z_T and Z_L), as shown in Fig. 6.

Signal propagation observed at the two measurement points (denoted as 1 and 2 throughout this analysis) is presented in Fig. 7, where the vertical axis symbolizes time and notations follow those of Section II. Ideally, if an impulse $\delta(t)$ is initially transmitted at point 1, a number of delayed replicas is received at point 2. In the setup of Fig. 6 however, the incoming signal is modified at point 1 by a factor of $U_{in} = Z_1/Z_g + Z_1$, where Z_1 is the aggregate impedance seen at point 1 by a signal propagating towards point 2.
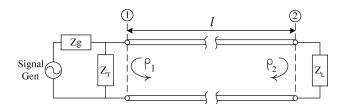

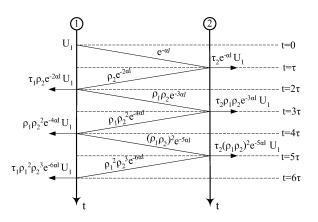Fig. 6. Cable-line measurement setup.

Fig. 7. Signal propagation on the line.

During the measurement process, the signals at the two points are acquired and processed in order to calculate the transfer function of the system between them. In order to compare measurements with the theoretical results, the theoretical transfer function of the corresponding system has to be determined. Based on Fig. 7, the two signals are expressed as:

$$s_1 = U_{in}.[\delta(t) + \sum_{i=1}^{L-1}\{\tau_1.\rho_1^{(i-1)}.\rho_2^{i}.e^{-2i\alpha l}.\delta(t - 2i\tau)\}]$$

$$s_2 = U_{in}.\sum_{i=1}^{L}\{\tau_2.(\rho_1.\rho_2)^{i}.e^{-(2i-1)\alpha l}.\delta(t - (2i - 1)\tau)\}$$

Consequently, the theoretical transfer function is given by:

$$TF_{1-2} = \frac{\sum_{i=1}^{L}\{\tau_2.(\rho_1.\rho_2)^{i}.e^{-(2i-1)\gamma l}\}}{1 + \sum_{i=1}^{L-1}\{\tau_1.\rho_1^{(i-1)}.\rho_2^{i}.e^{-2i\gamma l}\}}$$

The measurement procedure was based on the injection of tone signals at the center frequency of each subchannel. Measurements were collected at the two measurement points and the squared quotient of their FFT's was used to derive the respective transfer function. Theoretical and measurement-based transfer functions were found to be in satisfactory agreement. The comparison was repeated for different termination impedances Z_T and Z_L and different cable lengths. Typical results of the transfer function magnitude between points 1 and 2 are demonstrated in Fig. 8 for l=12.50 m and different impedances.

References

[1] S. Gardner, "The homeplug standard for powerline home networking," in *Proc. ISPLC'01*, Malm, Sweden, 2001, pp. 67–72.

[2] D. Liu, B. Flint, B. Gaucher, and Y. Kwark, "Wide band ac power line characterization," *IEEE Trans. Consumer Electronics*, vol. 45, no. 4, pp. 1087–1097, 1999.

[3] M. H. L. Chan and R. W. Donaldson, "Attenuation of communication signals on residential and intra-building power-distribution circuits," *IEEE Trans. Electromagnetic Compatibility*, vol. 28, no. 4, pp. 220–230, November 1986.

[4] H. Philips, "Modeling of powerline communication channels," in *Proc. ISPLC'99*, Lancaster, UK, 1999, pp. 14–21.

[5] M. Zimmermann and K. Dostert, "A multipath model for the powerline channel," *IEEE Trans. Communications*, vol. 50, no. 4, pp. 553–559, April 2002.

[6] F. Issa and A. Abdouss, "Indoor plc network simulator," in *Proc. ISPLC'02*, Athens, Greece, 2002, pp. 36–39.

[7] M. Sebeck and G. Bumiller, "Power-line analysing tool for channel estimation, channel emulation and noise characterisation," in *Proc. ISPLC'01*, Malm, Sweden, 2001, pp. 29–34.

[8] D. Anastasiadou and T. Antonakopoulos, "Analytical computation of multipath components in the indoor power grid," in *Proc. ISCAS'03*, Bangkok, Thailand, May 2003.

[9] ——, "An experimental setup for characterizing the residential power grid variable behavior," in *Proc. ISPLC'02*, Athens, Greece, 2002, pp. 65–70.

[10] S. Tsuzuki, T. Takamatsu, H. Nishio, and Y. Yamada, "An estimation method of the transfer function of indoor power-line channels for japanese houses," in *Proc. ISPLC'02*, Athens, Greece, 2002, pp. 55–59.
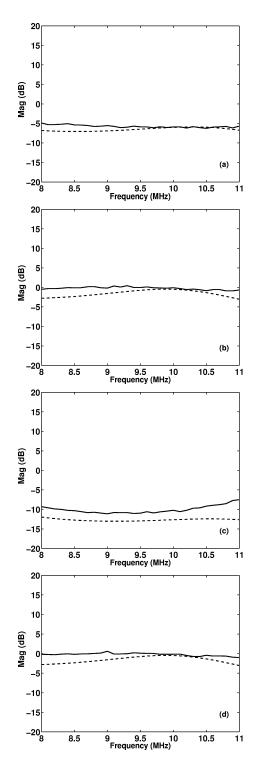
Fig. 8. Theoretical (solid line) and measured (dashed line) transfer functions of various impedances (in Ohms): (a) $Z_T = 95$, $Z_L = 51$, (b) $Z_T = 95$, $Z_L = 106$, (c) $Z_T = \infty$, $Z_L = 24$, (d) $Z_T = \infty$, $Z_L = 106$